Vibrational investigations of CO2-H2O, CO2-(H2O)2, and (CO2)2-H2O complexes isolated in solid neon

P. Soulard, B. Tremblay

Vibrational investigations of CO_2-H_2O, and CO_2-$(H_2O)_2$, and $(CO_2)_2$-H_2O complexes isolated in solid neon

P. Soulard, B. Tremblay*

Sorbonne Universités, UPMC Univ Paris 06, CNRS, UMR 8233, MONARIS, Case courrier 49, Université Pierre et Marie Curie, 4 place Jussieu, F-75005, Paris, France

Abstract

The van der Waals complex of H_2O with CO_2 has attracted considerable theoretical interest as a typical example of a weak binding complex with a dissociation energy less than 3 kcal/mol. Up to now, experimental vibrational data are sparse. We have studied by FTIR the complexes involving CO_2 and water molecules in solid neon. Many new absorption bands close to the well known monomers fundamentals give evidence for at least three $(CO_2)_n$-$(H_2O)_m$ complexes, noted n:m. Concentration effects combined with a detailed vibrational analysis allows for the identification of sixteen, twelve and five transitions for the 1:1, 1:2, and 2:1 complexes, respectively. Careful examination of the far infrared spectral region allows the assignment of several 1:1 and 1:2 intermolecular modes, confirmed by the observation of combinations of intra+intermolecular transitions, and anharmonic coupling constants have been derived. Our results demonstrate the high sensibility of the solid neon isolation to investigate the hydrogen-bonded complexes in contrast with the gas phase experiments for which two quanta transitions cannot be easily observed.

.

*Authors to whom correspondence should be addressed.

Electronic mail: benoit.tremblay@upmc.fr

KEYWORDS: water-CO_2 complex; van der Waals complex, Infrared Spectroscopy, Neon Matrix Isolation.

I. Introduction

The intermolecular interaction between water and carbon dioxide is important in atmospheric systems because water and carbon dioxide are the third and fifth most abundant molecules in the atmosphere, respectively (1). Also, the van der Waals complex of H_2O with CO_2, as a typical example of a weak binding complex, has attracted considerable theoretical interest and thus has given rise to many theoretical (2-20) and experimental studies (21-33).

The experimental contributions are in matrix isolation (21-27) and in gas phase by microwave spectroscopy (28-31), diode laser (32) and optothermal spectroscopy (33). Previous theoretical calculations (9) predict a planar T-shaped complex with C_{2v} symmetry as the most stable structural form and confirmed in gas phase by microwaves study (28), whereas a perpendicular form slightly tilted T-shaped structure with C_s symmetry was recently proposed (15) and potentially observed (24). For the 2:1 and 1:2 complexes, the only experimental data are obtained by microwaves spectroscopy (31,32) and these species have been the subject of a fewer number of theoretical studies (3,4,8,10,11,14,15,20) in comparison to CO_2-H_2O. Very little IR spectroscopic data for CO_2-H_2O system is available in the gas phase due probably to the weak binding energy.

In matrix experiments, the perturbation induced by heavy rare gases (Ar, Kr, Xe) or nitrogen or oxygen cannot be neglected for a weak binding complex **(**34**)**, and the use of less perturbing material, such as solid para-hydrogen (35) or Ne is essential. For example, the calculated binding energy values, in kcal/mol, for CO_2 and H_2O complexes with Ne, Ar, and N_2 are 0.3, 0.6, 0.9 and 0.19, 0.41, 1.3, respectively (36-40). The calculated value for the CO_2-H_2O complex is around 3 kcal/ mol with the CCSD(T) method (5,9,19). The binding energy of the Ne-H_2O and Ne-CO_2 complexes is 10% or less that of the calculated value for the H_2O-CO_2 complex, whereas the effect due to Ar and N_2 are 20-40%. This general trend from the

neon to the other rare gas atoms with increasing mass is well documented in the literature (34).

We have studied the CO_2-H_2O, CO_2-$(H_2O)_2$, and $(CO_2)_2$-H_2O complexes in neon isolation matrix to minimize the matrix effect and to obtain new vibrational data from 50 to 7000 cm^{-1} extending the spectral range up to the near infrared.

After a brief description of the experimental conditions, experimental spectra will be presented, an assignment of the different bands will be proposed and a comparison with previous results and theoretical studies will be discussed.

II. Experimental

Samples were prepared in a closed-cycle helium cryostat (Cryomech PT-405) by slow deposition (2 to 15 mmol/h) of CO_2.H_2O-neon mixtures on one side of a highly polished, rhodium-plated copper mirror maintained at 3K in most of the experiments and all the spectra have been recorded at 3 K. The temperature was measured using silicon diodes and the thermal annealing in the range 9-12K was regulated by a Neocera LTC-II temperature controller. The neon/CO_2 mole ratio varied between 200 and 60000, and the neon/water mole ratio varied between 100 and 2000 but variable desorption of water from the stainless steel vacuum line precluded accurate concentration measurements. Absorption spectra were recorded between 50 and 7000 cm^{-1} on the same sample using a Bruker 120 FTIR spectrometer equipped with suitable combinations of light sources (globar, W filament), beamsplitters (composite, KBr/Ge, Si/CaF_2, TiO_2/Quartz) and detectors (liquid N_2-cooled InSb, liquid N_2-cooled HgCdTe photoconductor, liquid He-cooled Si-B bolometer, room temperature Si photodiode). The resolution was generally fixed to 0.1 cm^{-1}. Natural water sample was degassed under vacuum before use. By analogy with the observations made for

N_2-doped Ar matrices (41), we have observed very weak absorptions assigned to $(H_2O)_m(N_2)_m$ complexes and we can estimate a amount of atmospheric impurities less than 30 ppm. Ne (Air Liquide, 99.995 % purity) and CO_2 (Air Liquide, 99.9 % purity) were used without purification.

III. Spectral data and assignments

The infrared absorptions of the H_2O monomer, dimer and trimer trapped in solid neon are well known for the fundamental modes, and for many overtones and combinations (42,43). Many data are available for the CO_2 monomer and dimer in solid argon and neon (44-46).

The experiments were conducted with different concentration ratios of CO_2/H_2O/Ne gas mixture to identify the transition of the n:m complexes. To identify first the 1:1 complex, experiments were performed using low concentration, typically CO_2/H_2O/Ne=0.02/0.5/1000, and for 1:m and n:1 complexes, using CO_2/H_2O/Ne=1/2-10/1000 and 2-6/2/1000, respectively. The complexes will be presented by considering absorptions due to the perturbed CO_2 and H_2O molecules. Figures 1-7 illustrate the IR spectra in different frequency ranges. Table I summarizes our measured vibrational frequencies of $(CO_2)_n$-$(H_2O)_m$ complexes.

A. CO_2 spectral regions

New intense absorptions at 2348.2 and 2348.8 cm^{-1} with an intensity ratio of 4/1, just above the $^{12}CO_2$ ν_3 band, are assigned to the ν_3 asymmetric vibration of $^{12}CO_2$ complexed with one water molecule (Fig 1). The isotopic counterparts $^{13}CO_2$:H_2O are also detected at 2282.5 and 2283.1 cm^{-1} as expected near the $^{13}CO_2$ ν_3 at 2282.2 cm^{-1}. Also, addition of H_2O to highly diluted CO_2 gives rise to new features located at 2350.2 and 2351.6 cm^{-1}, with an

intensity ratio of 8/1. We attributed these bands to the 1:2 complex since their intensities follow those of the H_2O dimer. Similarly for the 1:1 complex, we observe the $^{13}CO_2$-$(H_2O)_2$ complex at 2284.5 cm^{-1}. Conversely when the CO_2 concentration becomes higher than H_2O concentration we observe, near the CO_2 dimer bands at 2349.7, 2350.8, and 2352.2 cm^{-1}, a new band at 2349.3 cm^{-1} attributed to a 2:1 complex. Annealing effects or sample deposition at 6 K confirm these attributions for the 1:2 and 2:1 species. The observed frequencies for these complexes are summarized in the Table I.

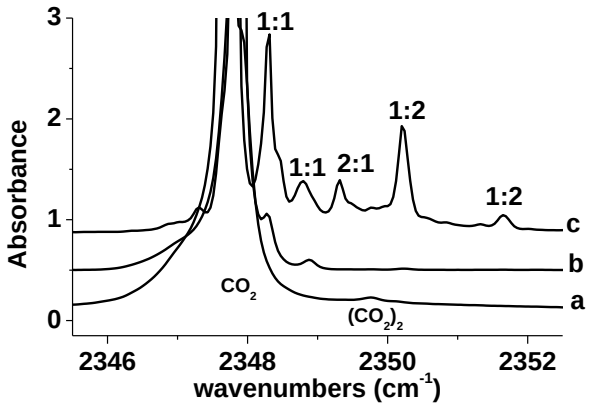

FIG. 1. Spectra in the CO_2 antisymmetric stretching (ν_3) region at 3K deposition, with different CO_2/H_2O/Ne concentration ratios. (a): 0.1/0/1000, (b): 0.016/1/1000, (c): 0.1/1/1000.

In the $^{12}CO_2$ ν_2 region, characterized for the monomer by very strong absorptions at 668.4 and 667.7 cm^{-1}, two strong features at 672.2 and 658.7 cm^{-1} appear when the two partners are deposited and are assigned to the bending vibration of $^{12}CO_2$ perturbed by H_2O (Fig 2) of the 1:1 complex. These bands behaved as the strong 1:1 band at 2348.2 cm^{-1} after concentration changes. We also observe the isotopic counterpart $^{13}CO_2$ of these bands at 653.1 and 640.2 cm^{-1}. Like in the $^{12}CO_2$ ν_3 region, we also see 1:2 and 2:1 absorptions at 653.8 and 670.6 cm^{-1}, and at 671.5, 663.5, and 656.0 cm^{-1}, respectively. At higher water concentration, two bands at 656.8 and 670.4 cm^{-1} are assigned to the 1:3 complex as these bands follow the H_2O trimer bands variation (Fig 1 and Table I).

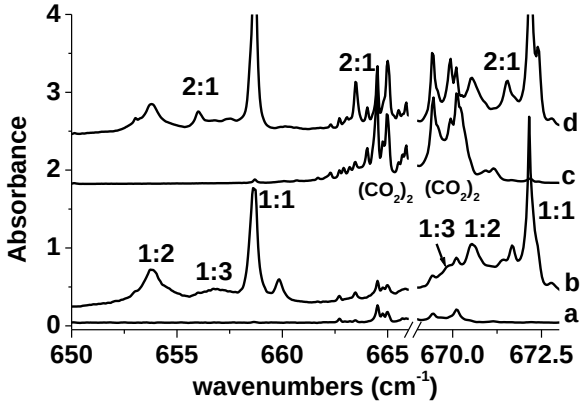

FIG. 2. Spectra in the CO_2 bending mode (ν_2) region with different CO_2/H_2O/Ne concentration ratios.
(a): 2/0/1000 at 3K deposition, (b): 1/20/1000 at 3K deposition, (c): 6/0/1000 at 6K deposition followed by annealing at 11K, (d): 3/1/1000 at 6K deposition followed by annealing at 11K.

Table I: Observed frequencies (cm^{-1}) and assignments for $(CO_2)_n$-$(H_2O)_m$ complexes.

n:m complex	Assignment	Observed frequencies	Relative intensity[a]
1:1	ν_i [b]	102.8	30
1:1	ν_i	167	
1:2	ν_i	195	
1:2	ν_i	222	
1:2	ν_2	653.8, 670.6	
1:3	ν_2	656.8, 670.4	
CO_2	ν_2	668.4, 667.7	
$(CO_2)_2$	ν_2	670.1, 664.5	
1:1	ν_2	672.2 , 658.7	20
2:1	ν_2	671.5, 663.5, 656.0	
1:1	ν_2	1595.2	9
1:2	ν_2	1597.8, 1612.3	
2:1	ν_2	1596.6	
H_2O	ν_2 (nrm [c])	1595.6	
$(H_2O)_2$	ν_2 PA	1599.2	
$(H_2O)_2$	ν_2 PD	1616.5	
1:1	ν_2+103	1703.3	
1:1	ν_2+166	1764.2	
CO_2	ν_3	2347.8	
1:1	ν_3	2348.2, 2348.8	100
$(CO_2)_2$	ν_3	2349.7	
2:1	ν_3	2349.3	
1:2	ν_3	2350.2, 2351.6	
1:1	ν_3+103	2465	
1:1	ν_3+166	2515	
1:1	$2\nu_2$	3153.9	
1:2	$2\nu_2$	3178.5	

$(H_2O)_2$	$2\nu_2$ PD	3193.7		
1:3	OH_b	3443.6		
1:2	OH_b	3561.2		
$(H_2O)_2$	ν_1 PD	3590.5		
1:1	$\nu_1+\nu_3(CO_2)$	3607.6		
CO_2	$\nu_1+\nu_3(CO_2)$	3611.9		
1:2	OH_b	3639		
2:1	OH_b	3650.6		
$(H_2O)_2$	ν_1 PA	3660.6		
1:1	ν_1	3664.8		3
H_2O	ν_1 (nrm)	3665.4		
1:2	OH_f	3739.5		
2:1	OH_f	3750.6		
1:1	ν_3	3760.3,	3754.5	25
$(H_2O)_2$	ν_3 PA	3763.5		
$(H_2O)_2$	ν_3 PD	3733.7		
H_2O	ν_3 (nrm)	3761.0		
1:2	OH_b +195	3851		
1:2	OH_b +222	3851		
1:1	ν_3 +103	3876		
1:1	ν_3 +166	3923		
1:2	$OH_b+\nu_2$	5153.5		
1:1	$\nu_2+\nu_3$	5320.2		

[a]band intensities relative to CO_2 ν_3 ($I\nu_3$=100) for the 1:1 complex.

[b]ν_i : frequencies of the intermolecular modes

[c]nrm: nonrotating monomer of H_2O (see text)

B. H_2O spectral regions

Near the ν_2 bending mode of the nonrotating monomer (nrm) (47) H_2O at 1595.6 cm^{-1} (Fig. 3), a new band appears at 1595.2 cm^{-1} when CO_2 is added to H_2O, and assigned to the 1:1 complex since this band behaved as the other 1:1 bands after concentration changes. Also, after studying the intensity variations of the three bands at 1596.6, 1597.8, and 1612.3 cm^{-1} over a wide concentration range, we find that the first band has a linear dependence, and the two others have a quadratic dependence, with regard to the water concentration. Varying the CO_2 concentration, however, the band at 1596.6 cm^{-1} has a quadratic dependence, whereas the bands at 1597.8 and 1612.3 cm^{-1} have a linear dependence. This shows that the band at 1596.6

cm^{-1} is the signature of the 2:1 complex, and the two bands at 1597.8 and 1612.3 cm^{-1} are the signatures of the 1:2 complex. Thermal annealing at 12 K permits diffusion of the molecules in the sample and enhances the intensity of the bands of the 0:2, 2:0, 1:2, and 2:1 complexes. We observe that the three bands at 1596.6, 1597.8, and 1612.3 cm^{-1} increase for the first one as the CO_2 dimer and for the two others as the H_2O dimer. This annealing effect confirms the stoichiometry of the 2:1 and 1:2 complexes.

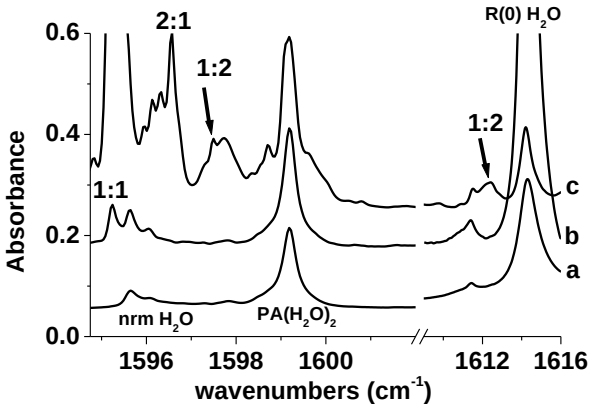

FIG. 3. Spectra in the H_2O bending mode (ν_2) region, with different CO_2/H_2O/Ne concentration ratios.
(a): 0/1/1000 at 3K deposition, (b): 0.016/1/1000 at 3K deposition, (c): 0.1/1/1000 at 3K deposition, (d): 3/0.3/1000 at 6K deposition followed by annealing at 12K.

We observe a new band at 3178.5 cm^{-1} attributed to $2\nu_2$ of 1:2 complex in the region of the $2\nu_2$ first overtone of the bending mode of the H_2O dimer (the proton donor (PD) and the proton acceptor (PA) bands at 3193.7 and 3163.0 cm^{-1}, respectively (36)). At weaker H_2O concentration a new band at 3153.9 cm^{-1} is assignable to $2\nu_2$ of 1:1 complex (Table I).

In the ν_1 symmetric O-H stretching region characterized by the absorption of the PA molecule of the water dimer at 3660.6 cm^{-1}, a shoulder near the ν_1 nrm at 3665.5 cm^{-1} appears and becomes a strong band when the concentration of the two partners is increased (Fig 4). After subtraction of the water monomer spectrum, this band is located at 3664.8 cm^{-1} and

assigned to the ν_1 symmetric O-H stretching mode of H_2O perturbed by the CO_2 complexation.

At higher water concentration, two bands appear at 3561.2 and 3639 cm^{-1} in the ν_1 region of the PD molecule of the water dimer at 3590.5 cm^{-1} (Fig 4 and Table I). These bands are correlated and so are attributed to the 1:2 complex, and precisely to the bonded OH stretching (OH_b). We also observe a band at 3443.6 cm^{-1} attributed to the 1:3 complex since these bands follow the H_2O trimer bands variation. At higher CO_2 concentration, a band attributed at the 2:1 complex appears at 3650.6 cm^{-1}. Finally, in the region of the CO_2 combination band $\nu_1+\nu_3$, observable at 3611.9 cm^{-1}, we attribute the band at 3607.6 cm^{-1} to the same combination of the 1:1 complex.

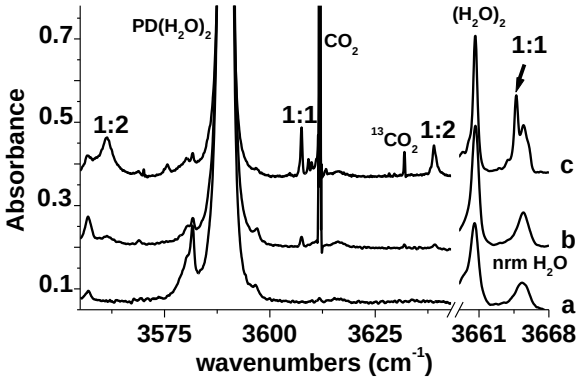

FIG. 4. Spectra in the 3550-3670 cm^{-1} region at 3K deposition with different $CO_2/H_2O/Ne$ concentration ratios. (a): 0/0.6:1000, (b): 0.1/0.6/1000, (c): 1/0.6/1000.

In the ν_3 asymmetric O-H stretching region characterized by the absorptions of the PD and PA molecule of the water dimer at 3733.7 and 3763.5 cm^{-1}, respectively, and the ν_3 of nrm at 3759.5 cm^{-1} (Fig. 5a), the 1:1 complex is characterized by two peaks at 3760.3 and 3754.5 cm^{-1} (Fig. 5b), with an intensity ratio of 6/1. Upon annealing at 12 K (Fig. 5c), only the band at 3760.3 cm^{-1} remains intense, which characterizes the most stable site for this mode. A shoulder at 3739.5 cm^{-1} on the right side of the water dimer band is attributed at the 1:2 complex, precisely at the free OH stretching (OH_f). We also see a band at 3750.6 cm^{-1} due

to the 2:1 complex, and all observed frequencies for these complexes are summarized in the Table I.

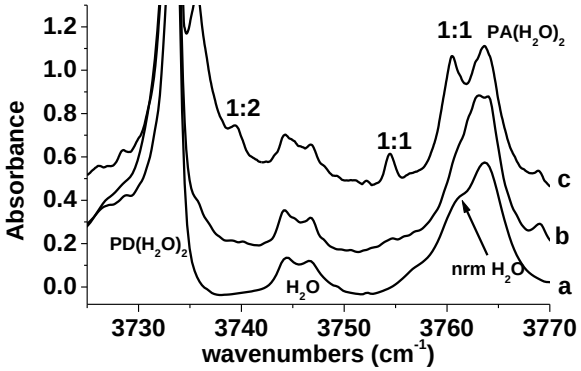

FIG. 5. Spectra in the 3725-3770 cm^{-1} region at 3K deposition with different CO_2/H_2O/Ne concentration ratios. (a): 0.1/0.6/1000, (b): 1/0.6/1000, (c): 1/0.6/1000 followed by annealing at 12K.

C. Intermolecular vibrations

Recently, Andersen and coworkers published a communication where far infrared spectra from 60 to 180 cm^{-1} are reported for the 1:1 complex in solid neon (21). They observed two intermolecular vibrations, the H_2O wagging and H_2O rocking at 101.6 and 166.6 cm^{-1}, respectively. With the HDO isotope, they observed a third band at 128.4 cm^{-1}, attributed to the intermolecular H_2O torsion (this band is infrared inactive with the natural isotope). We investigate the far infrared region and a well-defined band at 102.8 cm^{-1} was found as shown in figure 6. We also observe a band at 167 cm^{-1} as shown more precisely on the subtraction spectrum in figure 6c. These bands are in agreement with the recent study in far infrared. As our samples have been obtained with high concentration of the two partners, contrary to Andersen's experiments, we observe two additional bands at 195 and 223 cm^{-1} attributed to 1:2 complex after studying the concentration dependence of the absorption signals over a very wide range.

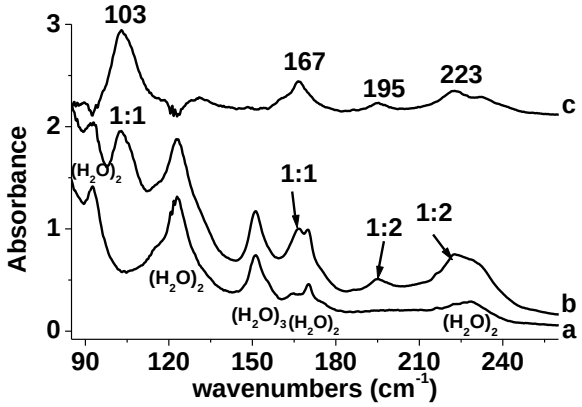

FIG. 6. Spectra in the 80-260 cm^{-1} region at 3K deposition with different CO_2/H_2O/Ne concentration ratios. (a): 0/1/1000, (b): 3/3.8/1000, (c): subtraction of spectra (b)-(a)

D. Multi quanta transitions

Many weak and broad bands are spread over 100 to 160 cm^{-1} above fundamental absorptions of the intramolecular mode of the 1:1 complex. Two bands appear at 1703.3 and 1764.2 cm^{-1} (Fig 7), above the H_2O ν_2 region, and are separated by about 60 cm^{-1} The similar observation can be done above the CO_2 ν_3 region at 2465 and 2515 cm^{-1}, separated by 50 cm^{-1}, and above the H_2O ν_3 region, at 3876 and 3923 cm^{-1} separated by 50 cm^{-1}. We attribute these to the combinations ν_{intra}+103 and ν_{intra}+167 where ν_{intra} corresponds successively to H_2O bending mode (ν_2), CO_2 asymmetric mode (ν_3), and H_2O asymmetric mode (ν_3). For the 1:2 complex, we observe a weak band at 3851 cm^{-1} that can be assigned to a combination between the 1:2 OH_b at 3639 cm^{-1} and one of the two intermolecular bands at 195 and 223 cm^{-1}. In the $\nu_1+\nu_2$ and $\nu_2+\nu_3$ H_2O regions, we observe two bands at 5320.2 and 5153.5 cm^{-1}, which can be attributed to the 1:1 and 1:2 complexes, respectively.

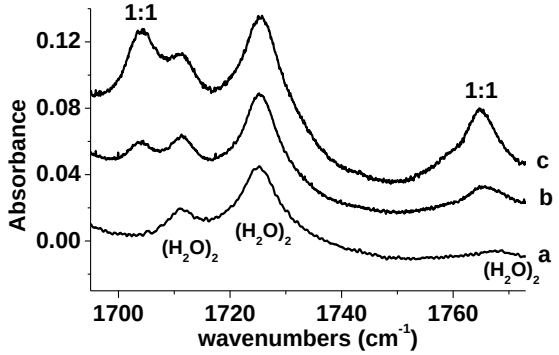

FIG. 7. Spectra in the 1695-1772 cm^{-1} region at 3K deposition with different $CO_2/H_2O/Ne$ concentration ratios. (a): 0.1/0.6/1000, (b): 1/0.6/1000, (c): 3/3.8/1000.

IV. Vibrational assigments and discussion

A. CO_2-H_2O complex

From the concentration effects, the position of seven fundamental transitions and nine overtones or combination absorption bands have been clearly established to the 1:1 complex. The fundamental bands of 1:1 complex are unambiguously assigned thanks to the previous matrix studies (22-27). We can observe that the H_2O vibrational modes and the ν_3 of CO_2 in the 1:1 complex are close to that of each monomer, characterizing a weakly bound van der Waals complex. In all the text, the frequency shifts are defined by $\Delta\nu=\nu_{monomer} - \nu_{complex}$.

It is difficult to compare the results from one matrix to another because many absorptions are split by the presence of multiple trapping sites which is often encountered in matrix isolation. For example, in argon, the CO_2 ν_3 is split in two sites at 2339.3 and 2344.8 cm^{-1} (25), but the 1:1 absorption has only a band at 2340.2 cm^{-1}, for a frequency shift of +0.9 and -4.6 cm^{-1}, depending on the monomer's band used as reference. In solid N_2 (24), the frequency shift is +2.0 cm^{-1}, and in neon, corresponding to the two bands observed for the 1:1 complex, the shifts are +0.4 and +1.0 cm^{-1}. We cannot explain why we have two bands for this vibrational mode. As the two bands have always the same intensity variation, whatever

the temperature deposition, they are not different sites. We cannot exclude the existence of two structures for the 1:1 complex, a planar T-shaped complex with C_{2v} symmetry and a perpendicular form slightly tilted T-shaped structure with C_s symmetry, with two very close CO_2 stretching modes since three works have suggested this possibility (8, 22, 24).

Several ab initio calculations predict a T-shaped geometry as the minimum for the 1:1 complex (2-20). Unfortunately, all the studies for the values of frequencies are at the harmonic level, except one (11). But in this latter study, the anharmonic calculations obtained using the CC-VSCF method reproduce badly the monomer frequencies. Because the comparison of anharmonic and, of course, harmonic frequencies with the experimental data is not possible, we will use the frequency shift between the monomer and the complex. The theoretical studies are at the MP2/aTZ level except one, which uses the CCSD(T) method (5), and the calculated frequencies are the same. We compare our experimental results with the work (3) giving the set of calculated frequencies for the entire observed complexes. In Table II we give a comparison of the frequencies shifts between CO_2 or H_2O monomer and complexes for observed and calculated data (3).

Table II: Comparison of frequencies shifts ($\Delta\nu=\nu_{monomer} - \nu_{complex}$) between CO_2 or H_2O monomer and complexes for observed and calculated data (3).

	CO_2				**H_2O**					
n:m	**ν_2**		**ν_3**		**ν_2**		**ν_1**		**ν_3**	
	exp	**theo**	**exp**	**theo**	**exp**	**theo**	**exp**	**theo**	**exp**	**theo**

1:1[a]	-4, +9	-4, +10	-0.4 -1	-2	-0.4	+1	+0.8	+6	+0.7	+7
2:1	-3.5, +4.5, +12	+1, -1, +6, +13	-1.5	0, -5	+1.0	+2	+15	+15	+9	+16
1:2[b]	-2.6, +14.2	-2, +13	-2.4 -3.8	-7	*+1.4* *+3.2*	*+2* *+1*	*+29.3* *+21.6*	*+34* *+26*	*+24*	*+16*

[a] Calculated values are given for the C_{2v} geometry of the 1:1 complex
[b] For the H_2O vibrations of the 1:2 complex, the frequencies shifts are given in comparison with the water dimer (italic values).

Theoretical frequency shifts are in good agreement for the CO_2 bending vibrations. For the H_2O regions, the experimental shifts are weaker than the calculated ones. But it is well-known that the frequency shift calculated within harmonic approximation for the O-H stretching (48) is greater than the experimental value. The calculated (9, 11) intensities of the modes for the 1:1 complex are in agreement with our experimental ones (table I).

One of the main results of this work is the observation of the multiquanta transitions. We clearly observe six combinations of intra+intermolecular modes (Table 1), four with water modes and two with CO_2 modes. These combinations show a small anharmonicity coefficient, in agreement with other water-molecule complexes (43,48). For the perturbed H_2O modes, we observe the $2\nu_2$ overtone and the $\nu_2+\nu_3$ combination at 3153.9 and 5320.2 cm^{-1}, respectively. We can deduce an anharmonicity coefficient x_{22} of -18.3 cm^{-1}, almost the same value than the H_2O monomer in gas phase (-18.9 cm^{-1}). Also, the ν_2 and ν_3 modes of the complex are very close to those of the H_2O monomer, but the value of the corresponding anharmonicity coefficient x_{23} equal to -35.3 cm^{-1} is surprisingly larger than the one in the H_2O monomer (-19.4 cm^{-1}). Note that the large decrease of $-x_{23}$ is correlated to the decoupling of the two OH oscillators, as suggested in the literature (36).

Besides, the existence of two structures for the 1:1 complex have been suggested from experimental data (22, 24) and calculations (8,24). However this assignment is questionable since a recent theoretical work (5) using CCSD(T) and CCSD(T)-F12 level is unable to identify this proposed asymmetric tilted “T-shape” structure of C*s* symmetry since in matrix it

is possible to stabilize less energy complexes in a local minimum due to presence of the matrix cage (49).

B. CO_2 -$(H_2O)_2$ complex

To our knowledge, our work is the first report on experimental vibrational data on the 1:2 complex apart from one previous investigation with microwave spectroscopy (30). In this study the structure is found to be cyclical with a relatively conserved H_2O dimer bond lengths. One water molecule is oxygen bound to the carbon atom of the CO_2 and is also hydrogen bonded to the oxygen of the second water molecule. The second water molecule is hydrogen bonded to one of the oxygens of the CO_2. There is relatively few works on the 1:2 complex (3,4,8,10,11,14,20) in contrast to the large number of theoretical studies on the 1:1 complex. For the bands in the OH stretching region, and in comparison with other hydrogen bonded systems (39,48), assignments of the two bands at 3561.2 and 3639 cm^{-1} to two bonded OH stretching (OH_b) vibrations is straightforward. The frequency shifts in italics in Table II are calculated with respect to the frequencies of the H_2O dimer isolated in neon (42). The observed shifts relating to the ν_1 PA and PD H_2O dimer are +29.3 and +21.6 cm^{-1}, and +24 cm^{-1} for the shifts relating to ν_3 H_2O dimer. These shifts are well reproduced by the calculation at the MP2 level since the calculated values are 34, 26 cm^{-1}, and 16 cm^{-1}, respectively. For the H_2O bending, the observed shifts are +1.4 and +3.2 cm^{-1}, in good agreement with the calculated ones, +1 and +2 cm^{-1}, respectively (Table II).

For the CO_2 regions, the two bands at 2350.2 and 2351.6 cm^{-1}, having an intensity ratio of 8/1, are attributed to the 1:2 complex, with -2.4 and -3.8 cm^{-1} frequency shifts. We cannot explain why two bands are observed for this vibrational mode. Like the 1:1 complex, we cannot exclude a possible stabilization by the neon atoms of a metastable form for the 1:2

complex (8). As the structure for this form implies a very weak perturbation for the water modes, it is probably the reason why we only observe another signature in the CO_2 ν_3 region. Note that the calculated shift is overestimated in comparison with the experimental ones. For the CO_2 bending, the theoretical frequency shifts reproduce well the experimental observations (Table II).

The attribution of the two bands in the far-infrared at 195 and 223 cm^{-1} to the 1:2 complex is supported by calculated bands at 198 and 218 cm^{-1} (20). The observation of one combination between the band at 3639 cm^{-1} and one of these two bands lends support to at least one of these two bands belonging to the 1:2 complex. Note that these two bands are very close to those of the water dimer (42).

We have also observed another multiquanta transition for the 1:2 complex. A $2\nu_2$ overtone of the H_2O bending is located at 3178.5 cm^{-1}, between the $2\nu_2$ overtones of the PD and PA water dimer (36), with an anharmonicity coefficient x_{22} of -8.6 or -23.0 cm^{-1}, depending of the value of the ν_2 band used for the calculation (1597.8 or 1612.3 cm^{-1}), whereas the values are -17.7 and -19.7 cm^{-1} for PA and PD of the H_2O dimer, respectively. Since the $2\nu_2$ overtone is six time more intense for the PD water dimer, we can assume that the observed band is the first overtone of the 1612.3 cm^{-1} band, for a x_{22} value of -23.0 cm^{-1}.

The band at 5153.5 cm^{-1} is attributed to the $\nu_1+\nu_2$ combination of the water modes in the 1:2 complex since the sum 1612.3 + 3561.2 =5173.5 cm^{-1} gives a small anharmonicity coefficient of -19.8 cm^{-1}. In comparison, the same combination for the PD water dimer gives a coefficient of -15.8 cm^{-1}.

C. $(CO_2)_2$-H_2O complex

There are only three theoretical works on the 2:1 complex (3,4,15) and our work is the first report on experimental vibrational data on this complex. The structure investigated by

microwave spectroscopy (31) is found to be two parallel CO_2 molecules like for the CO_2 dimer (50) slightly tilted and a water molecule above, with the hydrogen atoms directed away from the CO_2-CO_2 plane. The theoretical studies find the same stable form as shown in microwave experiment. For the bands in the OH stretching region, and in comparison with the water monomer, the two bands at 3650.6 and 3750.6 cm^{-1} could be easily assigned to ν_1 and ν_3 vibrations. In comparison with the same modes in the 1:1 complex, these are red-shifted, by 10 and 14 cm^{-1}, respectively, indicating a higher perturbation. The H_2O bending is blue shifted by 1.4 cm^{-1}, and all the shifts with the H_2O monomer are well reproduced by the calculations (Table II).

For the CO_2 regions, a band at 2349.3 cm^{-1} was attributed to this complex, with a -1.5 cm^{-1} frequency shifts in comparison to the CO_2 monomer (Fig 1). This shift of 1.9 cm^{-1} is very close to the one between the CO_2 dimer and monomer, not surprisingly for a complex formed by a CO_2 dimer and a water molecule. For the CO_2 bending, the theoretical frequency shifts reproduce well the experimental observations (Table II).

V. Conclusion

For the first time, a neon matrix isolation study of the $(CO_2)_m$-$(H_2O)_n$ complexes has been carried out from the far to the near infrared spectral range. On the basis of concentration and annealing effects, a set of sixteen, twelve and five transitions for the 1:1, 1:2, and 2:1 complexes, respectively, has been identified. Careful examination of the far infrared region allows the assignment of four 1:1 and 1:2 intermolecular modes, confirmed by the observation of combinations of intra+intermolecular transitions. Our results show interestingly not only one but two quanta vibrational transitions for these complexes. These data may help in the detection of these relevant interstellar and atmospheric complexes (11). This work shows well

the importance of neon matrix isolation for the study of very weak binding complexes. Many weak vibrational modes can be observed and can be greatly useful for theoretical investigations, especially at the anharmonic level.

REFERENCES

[1]V. Vaida, J. Chem. Phys. **135**, 020901 (2011).

[2]J. Karssemeijer, G. A. de Wijs, H. M. Cuppen, Phys. Chem. Chem. Phys. **16**, 15630 (2014).

[3]K. S. Thanthiriwatte, J. R. Duke, V. E. Jackson, A. R. Felmy, D. A. Dixon J. Phys. Chem A **116**, 9718 (2012).

[4]I. K. Ortega, A. Maattanen, T. Kurten, H. Vehkamaki, Comp. Theor. Chem. **965**, 353 (2011).

[5]K. M. de Lange and J. R. Lane, J. Chem. Phys. **134**, 034301 (2011).

[6]R. J. Wheatley and A. H. Harvey, J. Chem. Phys. **134**, 134309 (2011).

[7]A. S. Tulegenov, Chem. Phys. Lett. **505**, 71 (2011).

[8]C. N. Ramachandran and E. Ruckenseil, Comput. Theor. Chem. **966**, 84 (2011).

[9]J. Makarewicz, J. Chem. Phys. **132**, 234305 (2010).

[10]K. H. Lemke and T. M. Seward, J. Geophys. Res., **113** D19304 (2008).

[11]G. M. Chaban, M. Bernstein, D. P. Cruikshank, Icarus **187**, 592 (2007).

[12]J. A. Altmann, T. A. Ford, J. Mol. Struct. (Theochem.) **818**, 85 (2007).

[13]A. L. Garden, J. R. lane, H. G. Kjaergaard, J. Chem. Phys. **125**, 144317 (2006).

[14]N.R. Jena, P. C. Mishra, Theor. Chem. Acc. **114**, 189 (2005).

[15]Y. Danten, T. Tassaing, M. Bernard, J. Phys. Chem A **109**, 3250 (2005).

[16]M. Kieninger, O. N. Ventura, J. Mol. Struct. (Theochem.) **390**, 157 (1997).

[17]N. R. Zhang, D. D. Shillady, J.Chem. Phys. **100**, 5230 (1994).

[18]B. Jonsson, G. Karlstrom, H. Wennerstrom, Chem. Phys. Lett. **30**, 58 (1975).

[19]P. Ramasami, T. A. Ford, Mol. Phys. **112**, 683 (2014).

[20]M. T. Nguyen, M. H. Matus, V. E. Jackson, V. T. Ngan, J. R. Rustad, D. A. Dixon, J. Phys. Chem A **112**, 10386 (2008).

[21]J. Andersen, J. Heimdal, D.W. Mahler, B. Nelander, R. Wugt Larsen, J. Chem. Phys. **140**, 091103 (2014).

[22]X. Zhang, S. P. Sander, J. Phys. Chem A **115**, 9854 (2011).

[23]S. V. Ryazantsev, V. I. Feldman, J. Phys. Chem A **119**, 2578 (2015).

[24]A. Schriver, L. Schriver-Mazzuoli, P. Chaquin, E. Dumont, J. Phys. Chem A **110**, 51 (2006).

[25]X . Michaut, A.-M. Vasserot, L. Abouaf-Marguin, Low Temp. Phys. **29**, 852 (2003).

[26]T. Svensson, B. Nelander, G. Karlstrom, Chem. Phys. **265**, 323(2001).

[27]T. L. Tso, E. K. C. Lee, J. Phys. Chem **89**, 1618 (1985).

[28]K. I. Peterson, W. Klemperer, J. Chem. Phys. **80**, 2439 (1984).

[29]G. Colimberg, A. Bauder, N. Heineking, W. Stahl, J. Makarewicz, Mol. Phys. **93**, 215 (1998).

[30]K.I. Peterson, R. D. Suenram, F. J. Lovas, J. Chem. Phys. **94**, 106 (1991).

[31]K.I. Peterson, R. D. Suenram, F. J. Lovas, J. Chem. Phys. **90**, 5964 (1989).

[32]Y.Zhu, S. Li, C. Duan, J. Mol. Spectrosc. **283**, 7 (2013).

[33]P. A. Block, M. D. Marshall, L. G. Pedersen, R. E. Miller, J. Chem. Phys. **96**, 7321 (1992)

[34]M. E. Jacox, J. Phys. Chem. Ref. Data **32**, 1 (2003).

[35]L. Abouaf-Marguin, A.-M. Vasserot, C. Pardanaud, J. Stienlet, X . Michaut, Chem. Phys. Lett. **454**, 61 (2008).

[36]R. C., Erqiang Jiao, H. Zhu, Daiqian Xie, J. Chem. Phys. **133**, 104302 (2010).

[37]Y. Cui, H. Ran, D. Xie, J. Chem. Phys. **130**, 224311 (2009).

[38]S. Nasri, Y. Ajili, N. Jaidane, Y. N. Kalugina, P. Halvick, T. Stoecklin, M. Hochlaf, J. Chem. Phys. **142**, 174301 (2015).

[39] L. F. Roncaratti, L. Belpassi, D. Cappelletti, F. Pirani, and F. Tarantelli, J. Phys. Chem. A **113**, 52 (2009).

[40]A. S. Tulegenov, R.J. Wheatley, M. P. Hodges, A.H. Harvey, J. Chem. Phys. **126**, 094305 (2007).

[41]L. Abouaf-Marguin, A.-M. Vasserot, C. Pardanaud, X . Michaut, Chem. Phys. Lett. **447**, 232 (2007).

[42] Bouteiller , B. Tremblay, J.P. Perchard, Chem. Phys. **386**, 29 (2011).

[43]Tremblay, B. Madebène, M.E. Alikhani, J.P. Perchard, Chem. Phys. **378**, 27 (2010).

[44]A.-M. Vasserot, B. Gauthier-Roy, H. Chabbi, and L. Abouaf-Marguin, J. Mol. Spectrosc. **220**, 201 (2003).

[45] A. Schriver, L. Schriver-Mazzuoli, A. Vigasin, Vib. Spectrosc. **23**, 83 (2000).

[46] J. A. G. Castano, A. Rosana, M. Romano, J. Mol. Struct. **881,** 68 (2008).

[47]A. Engdahl, B. Nelander, B. J. Mol. Struct. **193**, 101 (1989).

[48] M. Cirtog, P. Asselin, P. Soulard, B. Tremblay, B. Madebène, M. E. Alikhani, R. Georges, A. Moudens, M. Goubet, T.R. Huet, O. Pirali, P. Roy, J. Phys. Chem. A **115**, 2523 (2011).

[49]L. Krim, X. Wang, L. Manceron, L . Andrews, J. Phys. Chem. A **109**, 10264 (2005).

[50] K W. Jucks, Z. S. Huang, R. E. Miller, G. T. Fraser, A. S. Pine, W. J. Lafferty, J. Chem. Phys. **88**, 2185 (1988).